J. Fluid Mech. (1980), *vol.* 101, *part* 4, *pp.* 705–720
Printed in Great Britain

Refraction–diffraction model for linear surface water waves

By CARLOS LOZANO

Applied Mathematics Institute and College of Marine Studies,
University of Delaware, Newark, DE 19711

AND PHILIP L.-F. LIU

School of Civil and Environmental Engineering,
Cornell University, Ithaca, NY 14850

(Received 9 November 1979 and in revised form 6 March 1980)

Based on the parabolic approximation, a refraction–diffraction model for linear water waves is developed. With the assumption that the water depth (refraction index) is slowly varying, the model equation describes the forward-scattered wavefield. Two examples are considered in particular: (i) wave diffraction by a long thin barrier on a uniform slope, and (ii) wave convergence over a semicircular step shoal. For the former problem, a similarity solution in terms of Fresnel integrals is obtained for the wavefield in the neighbourhood of the shadow boundary. For the latter problem, the resulting Schrödinger equation is solved numerically. The wavefield near the caustics as well as in the shadow region is obtained and compared with experimental data.

1. Introduction

The parabolic approximation has been used recently for studying wave forward-scattering problems in many physical fields such as optics, acoustic waves, electromagnetic waves and shallow water waves (e.g. Kriegsmann & Larsen 1978; Candel 1979; Mei & Tuck 1979). The approximation uses the fact that in the shadow boundary of a scatter, the modulation of wave amplitude is more rapid in the direction tangential to wave fronts than in the direction of wave rays; both wave fronts and rays are defined according to the geometrical ray theory. The disparity of scales leads to an approximate parabolic partial differential equation of the Schrödinger type, which describes the diffraction effects of slowly-varying refractive index in the forward scattered wave field. The primary advantage of this approximate approach is its relative simplicity in obtaining solutions either analytically or numerically.

In this paper, we derive formally a parabolic approximation to the linearized water wave theory via an asymptotic method. The index of refraction associated with the variation of bottom topography is always assumed to be slowly varying. The theory developed herein, unlike the work by Mei & Tuck (1980) and LeBlond & Mysak (1978), is not restricted to long-wave theory. The leading order parabolic approximation is applied to two physical problems: (i) the combined wave refraction and diffraction by a semi-infinite thin barrier installed on a uniformly sloping bottom, and (ii) the wave convergence over a stepped bottom. In the first problem a similarity solution for the wavefield is found in the neighbourhood of the shadow boundary where the classical wave ray theory fails. We find that when the curvature of the wave rays is

0022-1120/80/4599-2710 $02.00

ignored in the parabolic approximation, our solution reduces to that derived by Liu & Mei (1976). The curvature of the rays is important in the shallow water region for the case of a sloping beach. In the second problem, the parabolic approximation is used to study the wavefield in the vicinity of caustics, where the classical wave ray theory again fails. Numerical solutions are obtained for specific cases which were investigated experimentally by Whalin (1971). Good agreement between the experimental data and the present numerical results is observed.

2. General formulation

We first summarize the *linearized* governing equations and boundary conditions for small amplitude water waves (see, for example, Wehausen & Laitone 1960, p. 640). Cartesian co-ordinates $(\hat{x}, \hat{y}, \hat{z})$ are employed and fixed on the mean free surface $\hat{z} = 0$, where $\hat{z}$ is positive upwards. The undisturbed water depth is described by $\hat{z} = -\hat{h}(\hat{x}, \hat{y})$. Assuming that the fluid is inviscid and the wave motion is irrotational, we may introduce the velocity potential

$$\hat{\phi} = \hat{\phi}(\hat{x}, \hat{y}, \hat{z})\, e^{-i\hat{\omega}t}$$

for studying the time-periodic progressive waves with a given frequency $\hat{\omega}$. The gradient of the velocity potential gives the velocity vector.

The following dimensionless variables are adopted herein using the inverse of the frequency $\hat{\omega}^{-1}$ as the time scale and $\hat{g}/\hat{\omega}^2$ as the horizontal length scale:

$$\begin{gathered}(x, y, z) = (\delta\hat{x}, \delta\hat{y}, \hat{z})\,(\hat{\omega}^2/\hat{g}), \quad t = \hat{\omega}\hat{t}, \\ \phi = (\hat{\omega}^3/\hat{g}^2)\,\hat{\Phi}, \quad h = (\hat{\omega}^2/\hat{g})\,\hat{h};\end{gathered} \tag{2.1}$$

where all variables with circumflexes represent physical quantities and the small parameter δ characterizes the mild bottom slope.

In the first-order theory of small amplitude waves the velocity potential is governed by

$$\delta^2\Delta\Phi + \Phi_{zz} = 0, \qquad -h < z < 0; \tag{2.2}$$

$$\Phi_z - \Phi = 0, \qquad z = 0; \tag{2.3}$$

$$\Phi_z + \delta^2\nabla h \,.\, \nabla\Phi = 0, \qquad z = -h; \tag{2.4}$$

where $\Delta = \partial^2/\partial x^2 + \partial^2/\partial y^2$, $\nabla = (\partial/\partial x, \partial/\partial y)$ and the subscript z represents the differentiation with respect to z.

2.1. *Asymptotic ray theory*

The classical ray theory of water wave refraction on a slowly varying water depth is summarized herein. We assume that, for small δ, the velocity potential has the following asymptotic expression (Keller 1958):

$$\Phi \sim \{a(x, y) + \delta A^{(0)}(x, y, z) + O(\delta^2)\} \cosh\zeta \exp(i\delta^{-1}S) \tag{2.5}$$

where $\zeta = k(z+h)$ and $k(x, y)$ is the local wavenumber satisfying the dispersion relation

$$k \tanh kh = 1. \tag{2.6}$$

Using standard procedures, we obtain the following equations for the leading terms in (2.5):

$$(\nabla S)^2 = k^2, \tag{2.7}$$

$$(\nabla S) \cdot \nabla(a^2 I) + (\Delta S)\, a^2 I = 0; \tag{2.8}$$

where

$$I = \frac{\sinh 2kh}{2k} \frac{C_g}{C} \tag{2.9}$$

and C_g is the group velocity, while C is the phase velocity. Equation (2.7) is the eikonal equation of geometrical optics, the characteristics of which are called rays. Along a ray, the transport equation for the amplitude function a, (2.8), may be written (Keller 1958) as

$$a^2 I k\, d\tau = \tfrac{1}{2} a^2 \frac{C_g}{C} \sinh 2kh\, d\tau = \text{constant} \tag{2.10}$$

where $d\tau$ is the differential of the width of a strip formed by the rays. Equation (2.10) states that the energy flux is constant along a strip of rays.

For later use we should point out that the leading-order surface displacement, $\eta\,(= \hat{\eta}\hat{\omega}^2/\hat{g})$, can be expressed as

$$\eta = i\Phi(x, y, 0)\, e^{-it} = ia(x, y) \cosh kh \exp\left[i(\delta^{-1} S - t)\right](1 + O(\delta)) \tag{2.11}$$

in which the quantity $|a \cosh kh|$ is the leading-wave amplitude.

In view of (2.10) the ray theory breaks down, when the caustics ($d\tau = 0$) appear in the wave field. Otherwise, the leading-order ray theory is accurate up to $O(\delta)$ and the size of the domain of validity is $O(1/\delta)$ (Keller 1958).

2.2. *Propagation equations in the parabolic approximation*

For forward scattering problems where the diffraction effects of the refractive index become important, to extend the classical ray theory and its domain of validity we propose a velocity potential

$$\Phi \sim F(\rho, \sigma, z)\{a(x, y) + \delta A^{(0)}(x, y, z) + \delta^2 A^{(1)}(x, y, z) + \ldots\} \cosh \zeta e^{i\delta^{-1} S}, \tag{2.12}$$

where (ρ, σ) are curvilinear and orthogonal co-ordinates defined by the rays (ρ = constant) and the wave fronts (σ = constant). The corresponding physical variables $(\hat{\rho}, \hat{\sigma})$ are defined as (see (2.1))

$$(\rho, \sigma) = (\delta\hat{\rho}, \delta\hat{\sigma})\,(\hat{\omega}^2/\hat{g}). \tag{2.13}$$

Inserting (2.12) into (2.2)–(2.4), we obtain the following equations:

$$\begin{aligned}
&\{[k^2 - (\nabla S)^2]\, F + F_{zz}\}\, a \cosh \zeta \\
&+ \delta\{[A^{(0)}_{zz} \cosh \zeta + 2kA^{(0)}_z \sinh \zeta + i(\Delta S)\, a \cosh \zeta]\, F \\
&\quad + 2i\nabla S \cdot \nabla(a \cosh \zeta)\, F + 2i(\nabla S \cdot \nabla F)\, a \cosh \zeta \\
&\quad + 2[A^{(0)}_z \cosh \zeta + kA^{(0)} \sinh \zeta]\, F_z + A^{(0)} F_{zz} \cosh \zeta\} \\
&+ \delta^2\{[A^{(1)}_{zz} \cosh \zeta + 2kA^{(1)}_z \sinh \zeta + i(\Delta S)\, A^{(0)} \cosh \zeta]\, F \\
&\quad + 2i\nabla S \cdot \nabla(FA^{(0)} \cosh \zeta) + \Delta(Fa \cosh \zeta) \\
&\quad + 2[A^{(1)}_z \cosh \zeta + kA^{(1)} \sinh \zeta]\, F_z + A^{(1)} F_{zz} \cosh \zeta\} = 0, \quad -h \leqslant z \leqslant 0;
\end{aligned} \tag{2.14}$$

$$\begin{aligned}
&Fa[k \sinh kh - \cosh kh] + F_z a \cosh kh \\
&+ \delta\{F[A^{(0)}(k \sinh kh - \cosh kh) + A^{(0)}_z \cosh kh] + F_z A^{(0)} \cosh kh\} \\
&+ \delta^2\{F[A^{(1)}(k \sinh kh - \cosh kh) + A^{(1)}_z \cosh kh] \\
&+ F_z A^{(1)} \cosh kh\} + O(\delta^3) = 0, \quad z = 0;
\end{aligned} \tag{2.15}$$

$$aF_z+\delta\{[A_z^{(0)}+i(\nabla S\,.\,\nabla h)\,a]\,F+A^{(0)}F_z\}$$
$$+\delta^2\{F[A_z^{(1)}+i(\nabla S\,.\,\nabla h)\,A^{(0)}]+\nabla h\,.\,\nabla(Fa)$$
$$+F_zA^{(1)}\}+O(\delta^3)=0,\quad z=-h. \tag{2.16}$$

The complex-valued function F in (2.12) is intended to describe the deviations of the wave field manifest over a long distance from the classical ray theory due to effects of diffraction. We also anticipate that the diffraction factor F varies slowly within a wavelength but faster in the direction of a wave front than it does along a wave ray so that

$$\frac{\hat{\omega}^2}{\hat{g}}|F|\gg\left|\frac{\partial F}{\partial\hat{\rho}}\right|\gg\left|\frac{\partial F}{\partial\hat{\sigma}}\right|\quad\text{and}\quad O\left(\frac{\hat{\omega}^2}{\hat{g}}\left|\frac{\partial F}{\partial\hat{\sigma}}\right|\right)=O\left(\left|\frac{\partial^2F}{\partial\hat{\rho}^2}\right|\right).$$

Rewriting the above equations in terms of dimensionless variables from (2.13) we get

$$|F|\gg\delta\left|\frac{\partial F}{\partial\rho}\right|\gg\delta\left|\frac{\partial F}{\partial\sigma}\right|\quad\text{and}\quad O\left(\left|\frac{\partial F}{\partial\sigma}\right|\right)=O\left(\delta\left|\frac{\partial^2F}{\partial\rho^2}\right|\right). \tag{2.17}$$

This constitutes the basic assumption for the parabolic approximation. To incorporate these features into mathematics, we introduce a small parameter ϵ, which is a function of δ, and stretched co-ordinates

$$\tilde{\rho}=\epsilon^{-1}\rho,\quad\tilde{\sigma}=\epsilon\sigma,\quad\tilde{z}=\epsilon^2z \tag{2.18}$$

and write $\tilde{F}(\tilde{\rho},\tilde{\sigma},\tilde{z})=F(\epsilon\tilde{\rho},\epsilon^{-1}\tilde{\sigma},\epsilon^{-2}\tilde{z})$ with a formal expansion

$$\tilde{F}=\tilde{F}^{(0)}(\tilde{\rho},\tilde{\sigma})+\epsilon\tilde{F}^{(1)}(\tilde{\rho},\tilde{\sigma},\tilde{z})+O(\epsilon^2). \tag{2.19}$$

Substituting (2.18) into (2.17), we find that

$$\delta=\epsilon^3. \tag{2.20}$$

Therefore, the choice of the stretched co-ordinates (2.18) incorporated with the parabolic approximation allows us to examine the variations of the diffraction factor $\tilde{F}$ along the ray direction within a distance $O(\delta^{-\frac{1}{3}})$, since $\tilde{\sigma}=\delta^{\frac{1}{3}}\hat{\sigma}\hat{\omega}^2/\hat{g}$.

Inserting (2.18)–(2.20) into governing equations (2.14)–(2.16), we obtain, after some manipulations, a set of equations for a, $A^{(k)}$, and $\tilde{F}^{(k)}$ as power series in ϵ. The details of the resulting power series are presented in the appendix. Equating the coefficients of different power in ϵ of the power series to zero, we find that if the amplitude function $a(x,y)$ and the phase function S are precisely the same ones as described by classical ray theory, (2.6)–(2.8), the governing equations are satisfied up to $O(\epsilon^3)$. Equating the coefficients of $O(\epsilon^4)$ terms in the power series yields the leading-order parabolic approximation

$$2ik\tilde{F}_{\tilde{\sigma}}^{(0)}+\Delta_{(\tilde{\rho})}\tilde{F}^{(0)}=0 \tag{2.21}$$

where

$$\Delta_{(\tilde{\rho})}\tilde{F}^{(0)}=h_{(\rho)}^{-2}\frac{\partial^2\tilde{F}^{(0)}}{\partial\tilde{\rho}^2}+[h_{(\sigma)}\,h_{(\rho)}]^{-1}\left[\frac{\partial(h_{(\sigma)}h_{(\rho)}^{-1})}{\partial\tilde{\rho}}\right]\frac{\partial\tilde{F}^{(0)}}{\partial\tilde{\rho}}, \tag{2.22a}$$

$$\tilde{F}_{\tilde{\sigma}}^{(0)}=h_{(\sigma)}^{-1}\frac{\partial\tilde{F}^{(0)}}{\partial\tilde{\sigma}} \tag{2.22b}$$

and $h_{(\sigma)}$ and $h_{(\rho)}$ are the scale factors, giving the ratios of differential distances to the differentials of the co-ordinate parameters. Since the co-ordinates (ρ,σ) are orthogonal,

then $(ds)^2 = h_{(\sigma)}^2(d\sigma)^2 + h_{(\rho)}^2(d\rho)^2$; ds is the arclength differential. Equation (2.21) indicates that owing to diffraction the wave energy diffuses across the wave rays. Moreover, the effects of ray curvatures are included in the parabolic approximation. The remaining higher-order terms in the power series provide successive governing equations of *coupled* systems for the diffraction terms $\tilde{F}^{(k)}$ and the refraction terms $A^{(k)}$ (see appendix).

In summary, the leading-order velocity potential of the parabolic approximation is given as

$$\Phi = \tilde{F}^{(0)}(\tilde{\rho}, \tilde{\sigma})\, a(x,y)\,[1 + O(\delta^{\frac{1}{3}})] \cosh \zeta\, e^{i\delta^{-1}S} \tag{2.23}$$

where $a(x,y)$ and $S(x,y,t)$ are obtained from the ray theory, while the diffraction factor $\tilde{F}^{(0)}$ satisfies the Schrödinger equation (2.21). Note that the leading-order solution has a uniform error $O(\delta^{\frac{1}{3}})$ which is larger than that of the leading-order ray theory, $O(\delta)$. However, the size of the domain of validity for the parabolic approximation is greater than that of the ray theory. In § 3 we use the technique developed here to study the combined refraction and diffraction wave field in the neighbourhood of a thin barrier installed in a slowly varying water depth.

2.3. *Parabolic approximation near a caustic*

It is well-known that the wave ray theory fails near a caustic because the theory gives an infinitely high wave amplitude in the vicinity of the caustic. Moreover, there exists a shadow region on the other side of the caustic, where the wave amplitude is zero. Within the framework of *linear* wave theory this difficulty can be overcome by employing a uniform asymptotic theory (e.g. Chao 1971; Ludwig 1964; Shen & Keller 1975). Unfortunately, the numerical implementation of the uniform ray theory is usually very complicated for practical uses. In this section we intend to show that with a slight modification the parabolic approximation developed in the previous section can be used to compute easily the wavefield in the vicinity of a caustic.

For a given bottom topography $z = -h(x,y)$ the classical wave ray theory predicts the existence of a caustic in a certain region R. We introduce a modified topography $z = -\bar{h}(x,y)$ in the same region R such that the wave field associated to $\bar{h}$ can be described as

$$\bar{\Phi} = \bar{a}(x,y)\,[1 + O(\delta)] \cosh \bar{\zeta}\, e^{i\delta^{-1}\bar{S}}, \tag{2.24}$$

in the entire region R according to wave ray theory; no caustic exists. In (2.24) $\bar{a}$ and $\bar{S}$ are the amplitude function and phase function, respectively, and $\bar{\zeta} = C(z + \bar{h})$ with the wavenumber C satisfying the dispersion relation $\bar{k} \tanh \bar{k}\bar{h} = 1$. The difference between the actual bottom topography $z = -h$ and the modified topography $z = -\bar{h}$ is small so that

$$k^2 = \bar{k}^2 - \epsilon^4 V(x,y), \tag{2.25}\dagger$$

where k is the wavenumber associated with h, i.e. $k \tanh kh = 1$, and $V(x,y)$ is bounded as ϵ tends to zero. Now we can view the wave field in the neighbourhood of the caustic predicted by ray theory as the result of the diffraction of the refracted wave field $\bar{\Phi}$, (2.24), due to the topographical deviation, $h - \bar{h}$. In other words, we can approximate

† From the dispersion relation and (2.25), we deduce that $O(h - \bar{h}) = O([k - \bar{k}]/(dk/dh)_{\bar{h}}) = O(\epsilon^4 V/k(dk/dh)_{\bar{h}})$. It should be pointed out, however, that the shoreline singularity (Shen 1972) is not being studied here.

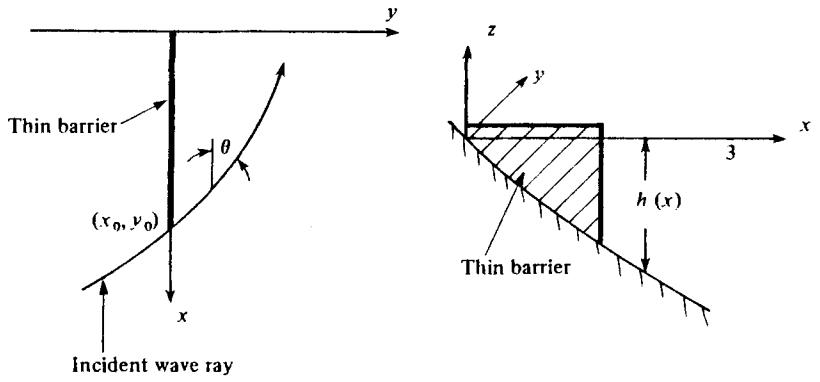

FIGURE 1. Sketch of the beach topography and the location of the thin barrier.

the leading-order velocity potential associated with the actual bottom topography $z = -h$ as follows:

$$\Phi \sim \bar{F}^{(0)}(\bar{\rho}, \bar{\sigma})\{\bar{a}\cosh\bar{\zeta}e^{i\delta^{-1}\bar{S}}\} \tag{2.26}$$

where $(\bar{\rho}, \bar{\sigma})$ are the stretched curvilinear co-ordinates associated to the ray pattern of $\bar{S}$. We remark here that any difference in a choice of $\bar{h}$ would lead to a different diffraction factor $\bar{F}^{(0)}$; there is, in other words, a trade-off between the wave refraction and wave diffraction. The governing equation for the diffraction factor $\bar{F}^{(0)}$ can be obtained by following the same procedure presented in the previous section with an exception that the bottom boundary condition must be evaluated as $z = -\bar{h}$. Thus

$$2i\bar{k}\bar{F}^{(0)}_{\sigma} + \Delta_{(\bar{\rho})}\bar{F}^{(0)} - V\bar{F}^{(0)} = 0. \tag{2.27}$$

The differences between the preceding equation and (2.21) are the appearance of the V term in (2.27) and the fact that the curvilinear co-ordinates $(\bar{\rho}, \bar{\sigma})$ are associated with the phase function $\bar{S}$. The true bottom topography enters into (2.27) in the term $V\bar{F}^{(0)}$. The wave behaviour near the caustic, including the shadow region, should be contained in the solution of $\bar{F}^{(0)}$.

We conclude this section with a remark that the leading-order approximation of the wave field given in (2.26) has a uniform error $O(\delta^{\frac{1}{2}})$ which is consistent with the uniform ray theory developed by Chao (1971, equation (16)). In view of the fact that it is relatively simple to solve (2.27) numerically, the parabolic approximation serves as a convenient alternative for describing the wave field near a caustic. Of course when the nonlinear effects become important, both uniform ray theory and the parabolic approximation need to be modified to accommodate the nonlinearity.

3. Combined refraction and diffraction by a thin barrier

As the first example for the parabolic approximation, we consider the combined diffraction and refraction wave field in the neighbourhood of an impervious barrier. The barrier with an infinitesimal thickness is installed on a mildly sloping beach as shown in figure 1. Using the co-ordinate system defined in this figure the leading-order solutions for wave refractions as given by ray theory are

$$a(x) = a_{\infty}\left[\frac{k}{k_{\infty}}\frac{\alpha_{\infty}}{\alpha}\frac{2k_{\infty}h_{\infty} + \sinh 2k_{\infty}h_{\infty}}{2kh + \sinh 2kh}\right]^{\frac{1}{2}}\frac{\cosh kh}{\cosh k_{\infty}h_{\infty}}, \tag{3.1}$$

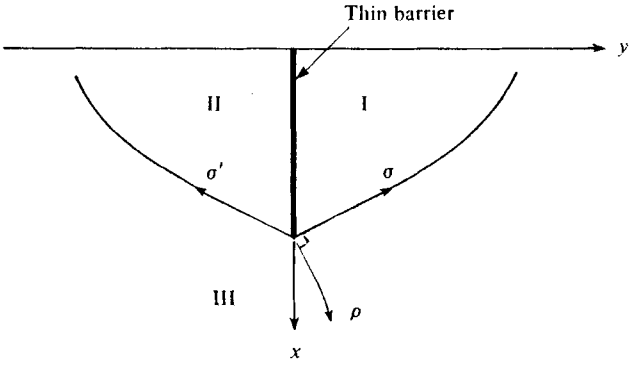

FIGURE 2. Separate regions according to geometrical optic theory.

$$S(x,y) = \beta y - \int^x \alpha\, dx, \tag{3.2}$$

where

$$\alpha(x) = k\cos\theta, \quad \beta = k(x)\sin\theta \equiv k_\infty \sin\theta_\infty. \tag{3.3}$$

are the x and y components of the local wavenumber vector $\mathbf{k}(x)$ and $\theta(x)$ is the angle of incidence. The subscript ∞ refers to infinity, where the water depth is h_∞. The orthogonal co-ordinates (ρ, σ) representing the rays and the phase lines can be written as

$$\begin{aligned} \rho &= (y - y_0) + \int_{x_0}^x \tan\theta\, dx, \\ \sigma &= (y - y_0) - \int_{x_0}^x \cot\theta\, dx, \end{aligned} \tag{3.4}$$

where (x_0, y_0) is chosen to be the location of the tip of the barrier. The rays are described by ρ = constants and the curve σ = constant describes a line of constant phase. For later use we observe that

$$h_{(\sigma)} = \sin\theta, \quad h_{(\rho)} = \cos\theta. \tag{3.5}$$

According to geometrical wave ray theory, the entire wave field can be divided into three regions (see figure 2). In the shadow region I, which is bounded by the critical incident wave ray $\rho = 0$ and the barrier, the wave action is zero. In the reflexion region II, which is bounded by the breakwater and the critical reflected wave ray $\rho' = 0$, the wave action is the super-position of the incident wave and the reflected wave. In the incident region III which is the complement of the shadow and reflexion region, the wave action does not feel the appearance of the barrier. Across the critical rays, $\rho = 0$ and $\rho' = 0$, the wave action experiences discontinuities, which suggest the invalidity of the geometrical ray theory in these neighbourhoods. To remedy this problem, Liu, Lozano & Pantazaras (1979) developed a uniform asymptotic theory. One of the disadvantages of this latter approach is the substantial amount of numerical work required in its implementation.

The problem can be solved approximately but efficiently, however, by adopting the parabolic approximations in the neighbourhood of the critical rays. We illustrate this point by considering only the downwave side of the barrier. To include the effects of diffraction, from (2.12) the leading-order potential can be written as

$$\Phi \simeq \tilde{F}^{(0)}\{a\cosh\zeta\}\exp(i\delta^{-1}S), \tag{3.6}$$

where a and S are given by (3.1) and (3.2), respectively. Substituting (2.22) and (3.5) into (2.21), we find that $\tilde{F}^{(0)}$ satisfies the following equation

$$2i\beta\cot^2\theta\frac{\partial\tilde{F}^{(0)}}{\partial\tilde{\sigma}}+\frac{\partial^2\tilde{F}^{(0)}}{\partial\tilde{\rho}^2}+\frac{1}{\sin 2\theta}\frac{\partial\theta}{\partial\tilde{\rho}}\frac{\partial\tilde{F}^{(0)}}{\partial\tilde{\rho}}=0. \tag{3.7}$$

An approximation proposed previously by Liu & Mei (1976) is the same as (3.7) except that in their work the last term on the left-hand side of (3.7) is missing. Keeping this term in the parabolic approximation, we have taken the curvature of rays and phase lines into consideration. It is easy to show that fron Snell's law (3.3) and the definition of the phase lines (3.4), the following is true:

$$O\left(\left|\frac{\partial\theta}{\partial\tilde{\rho}}\right|\right)=O\left(\epsilon\left|k^{-1}\frac{dk}{dx}\right|\right). \tag{3.8}$$

In the case of a shallow water waves, $1\cong k^2h$, we may rewrite (3.8) as follows:

$$O\left(\left|\frac{\partial\theta}{\partial\tilde{\rho}}\right|\right)=O\left(\epsilon\left|h^{-1}\frac{dh}{dx}\right|\right). \tag{3.9}$$

Therefore, the effects of the curvature of rays become increasingly important as waves propagate towards the shoreline.

Equation (3.7) may be rewritten in the following form

$$f\frac{\partial}{\partial\tilde{\rho}}\left(f\frac{\partial\tilde{F}^{(0)}}{\partial\tilde{\rho}}\right)+2i\beta f^2\cot^2\theta\frac{\partial\tilde{F}^{(0)}}{\partial\tilde{\sigma}}=0, \tag{3.10}$$

where

$$f=\exp\left[\int^{\tilde{\rho}}\frac{1}{\sin 2\theta}\frac{\partial\theta}{\partial\tilde{\rho}}\partial\tilde{\rho}\right]=(\tan\theta)^{\frac{1}{2}}. \tag{3.11}$$

Equation (3.10) is the same as that of Liu & Mei (1976) if $f\equiv 1$. We now replace the independent variables $(\tilde{\rho},\tilde{\sigma})$ by (ξ,ν), where

$$\nu=\frac{1}{\beta}\int_0^{\tilde{\sigma}}\tan\theta\,d\tilde{\sigma},\quad \xi=\int_0^{\tilde{\rho}}(\cot\theta)^{\frac{1}{2}}d\tilde{\rho}. \tag{3.12), (3.13}$$

Equation (3.10) becomes

$$\frac{\partial^2\tilde{F}^{(0)}}{\partial\xi^2}+2i\frac{\partial\tilde{F}^{(0)}}{\partial\nu}=0. \tag{3.14}$$

The boundary conditions for $\tilde{F}^{(0)}$ are

$$\begin{aligned}&\tilde{F}^{(0)}\to 1,\quad \xi\to\infty;\\ &\tilde{F}^{(0)}\to 0,\quad \xi\to-\infty.\end{aligned} \tag{3.15}$$

The similarity solution to (3.14) and (3.15) can be found in terms of Fresnel integrals,

$$\tilde{F}^{(0)}=2^{-\frac{1}{2}}\{[\tfrac{1}{2}+C(\xi/(\pi\nu)^{\frac{1}{2}}]+i[\tfrac{1}{2}+S(\xi/(\pi\nu)^{\frac{1}{2}})]\}\,.\,e^{-\frac{1}{4}i\pi}; \tag{3.16}$$

where

$$S(z)=\int_0^z\sin\left(\frac{\pi\tau^2}{2}\right)d\tau,\quad C(z)=\int_0^z\cos\left(\frac{\pi\tau^2}{2}\right)d\tau \tag{3.17}$$

are sine and cosine Fresnel integrals.

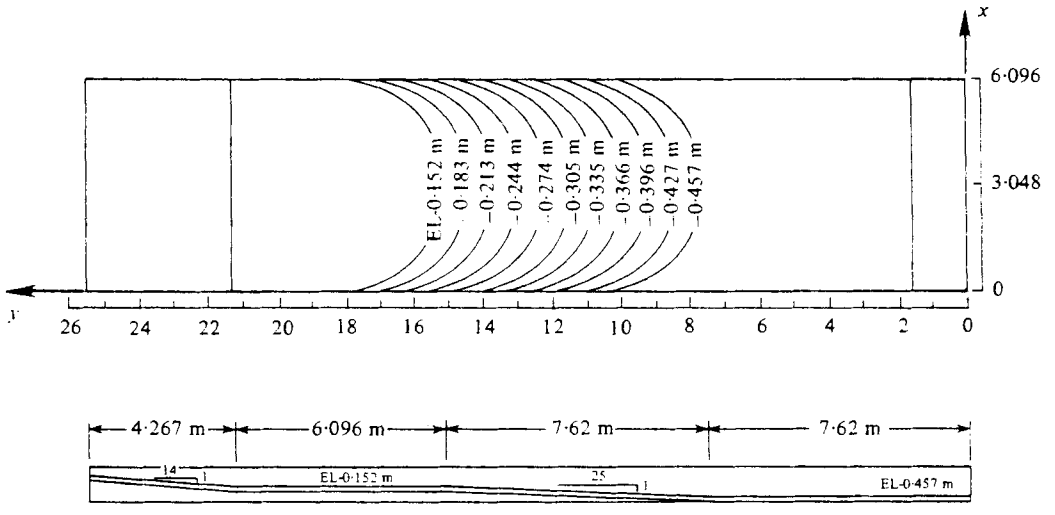

FIGURE 3. Wave-tank configuration.

From (3.16) it is clear that the boundary of the transition zone can be defined by $\xi/(\pi\nu)^{\frac{1}{2}} =$ constant, which is a sort of parabolic with the critical ray $\rho = 0$. as it axis. Within this transition zone the refracted–diffracted wave may be viewed as a refracted wave with modulated wave amplitude and phase both along and normal to the wave rays $\rho =$ constants. The diffraction factor $|\tilde{F}^{(0)}|$ diminishes monotonically for $\xi < 0$ (in shadow region), and approaches one as $\xi \to \infty$ (incident region) in an oscillatory manner.

4. Wave convergence due to bottom topography

In this section we demonstrate with an example how the parabolic approximation can be used to study a wave field where, according to classical ray theory, caustics appear owing to bottom topography. The set-up of Whalin's (1971) wave-tank experiments is used to define the example so that his experimental data can be used as a verification of the approximate theory.

Whalin's experiments were conducted in a wave tank with the horizontal dimensions 25·603 m × 6·096 m. A wave-maker was installed at the deep portion of the channel ($y = 0$). In the middle portion of the channel, 7·62 m $< y <$ 14·81 m, eleven semi-circular steps were evenly spaced and led to the shallower portion of the channel (figure 3). At the other end portion of the channel ($y >$ 21·34 m) a very shallow beach with $\frac{1}{14}$ slope was installed to dissipate (with the aid of wave absorber) most of the incoming wave energy and to reduce wave reflexions to minimum. The equations approximating the bottom topography are given as follows† (Whalin 1971):

$$h(x,y) = \begin{cases} 0{\cdot}4572 & (0 \leqslant y \leqslant 10{\cdot}67 - G(x)), \\ 0{\cdot}4572 + (G-y)/25 & (10{\cdot}67 - G \leqslant y \leqslant 18{\cdot}29 - G), \\ 0{\cdot}1524 & (18{\cdot}29 - G \leqslant y \leqslant 21{\cdot}34), \end{cases} \tag{4.1}$$

where

$$G(x) = [x(6{\cdot}096 - x)]^{\frac{1}{2}}, \quad 0 \leqslant x \leqslant 6{\cdot}096. \tag{4.2}$$

† In this section variables are dimensional (MKS system).

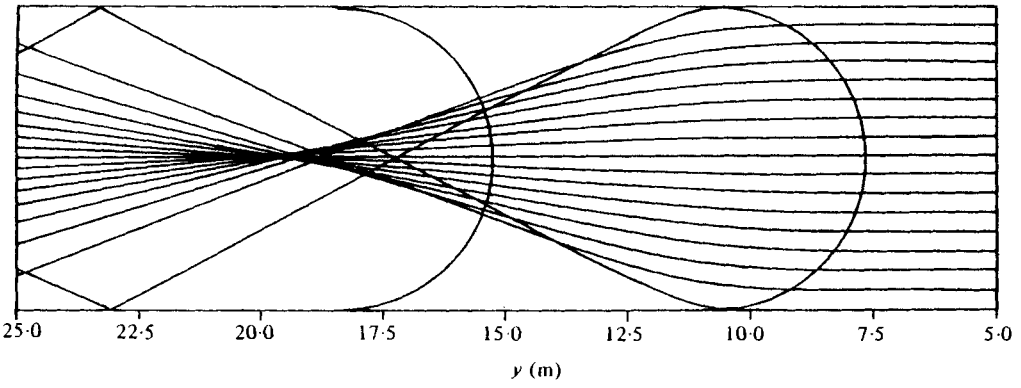

FIGURE 4. Convergence of wave rays for $T = 3$ s.

The bottom topography is symmetric with respect to the centre-line of the wave tank, $x = 3{\cdot}048$ m.

In Whalin's experiments simple harmonic waves with periods $T = 1$, 2, and 3 s, were generated. Owing to the mild slope ($\approx \frac{1}{25}$) the reflexions from topography were negligible. Using the classical ray theory described in § 2.1, we compute the wave ray patterns for $T = 3$ s (figure 4). It is apparent that the ray pattern possesses two line singularities (caustics) which merge at a singular point (cusp point: $y = 20$ m, $x = 3{\cdot}048$ m). The entire wave field can be divided into three subregions: (1) An incidence region bounded by the wave-maker, the lateral walls of the wave tank and the cusped caustic, (2) the shadow regions where no ray exists, and (3) a divergence region covered by rays emerging from the cusped caustic. The ray theory is clearly not applicable in the shadow region and in the neighbourhood of the cusped caustic.

To solve the problem by the parabolic approximation, we choose the modified bottom topography $\bar{h}$ as follows:

$$\bar{h}(x,y) = \begin{cases} 0{\cdot}4572 & (0 \leqslant y \leqslant 7{\cdot}62); \\ 0{\cdot}4572 - (y - 7{\cdot}62)/25 & (7{\cdot}62 < y \leqslant 15{\cdot}24); \\ 0{\cdot}1524 & (15{\cdot}24 < y < 21{\cdot}34). \end{cases} \tag{4.3}$$

The wave rays corresponding to the plane waves travelling on the ramp described by (4.3) are simply straight lines, $x = x_0$ ($0 \leqslant x_0 \leqslant 6{\cdot}096$). The wave action $a(x,y)$, which is the shoaling factor in this case, can be obtained readily from (2.10). Thus

$$\bar{a}(x,y) = \bar{a}_0(x,0)\left[\frac{C_g(x,0)}{C_g(x,y)}\right]^{\frac{1}{2}} \frac{\cosh \bar{k}_0 \bar{h}_0}{\cosh \bar{k}\bar{h}}, \tag{4.4}$$

where the subscript 0 denotes the physical quantities evaluated at the location of the wave-maker, i.e. $y = 0$. The corresponding phase function $\bar{S}(x,y)$ can be written as

$$\bar{S}(x,y) = \int_0^Y \bar{k}(y')\,dy' + \bar{S}_0, \tag{4.5}$$

where $\bar{k}$ satisfies the dispersion relation in terms of $\bar{h}$.

As discussed in § 2.3 the leading-order velocity potential corresponding to the true topography h described in (4.1) can be written as

$$\Phi \sim \bar{F}^{(0)}(\bar{\rho},\bar{\sigma})\{\bar{a}\cosh \bar{k}(z+\bar{h})\exp(i\delta^{-1}\bar{S})\},$$

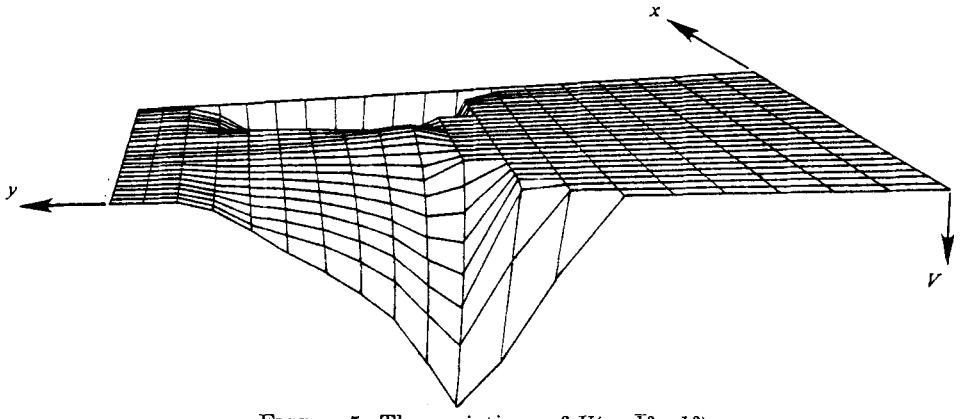

FIGURE 5. The variations of $V(=\bar{k}^2-k^2)$.

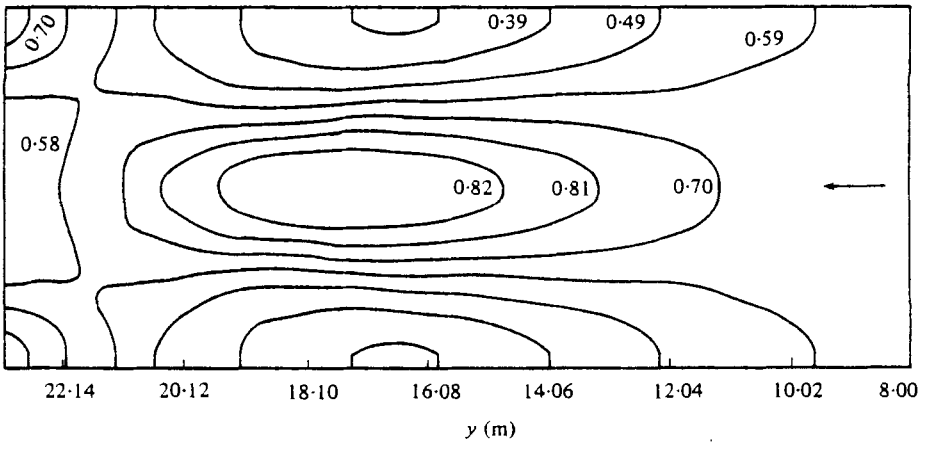

FIGURE 6. Contour lines of $|\bar{F}^{(0)}|^2$ for $T = 3$ s.

where $\bar{F}^{(0)}$ can be viewed as the diffraction factor caused by the topographical difference between h and $\bar{h}$. Since the background waves are plane waves and propagate in the y direction, $(\bar{\rho}, \bar{\sigma}) = (x, y)$ and the parabolic equation for the diffraction factor, (2.27), may be reduced to the Schrödinger equation in the following dimensional form:

$$2i\bar{k}\frac{\partial \bar{F}^{(0)}}{\partial y} = -\frac{\partial^2 \bar{F}^{(0)}}{\partial x^2} + V\bar{F}^{(0)}, \tag{4.6}$$

where

$$V(x, y) = \bar{k}^2 - k^2, \tag{4.7}$$

and k is the wavenumber associated with the true bottom topography $h(x, y)$ given by (4.1). The boundary conditions are

$$\bar{F}^{(0)}(x, 0) = 1, \quad 0 \leqslant x \leqslant 6{\cdot}096, \tag{4.8}$$

and

$$\frac{\partial \bar{F}^{(0)}}{\partial x} = 0, \quad x = 0,\ 6{\cdot}096. \tag{4.9}$$

The initial boundary-value problem described by (4.6)–(4.9) (y is a time-like variable)

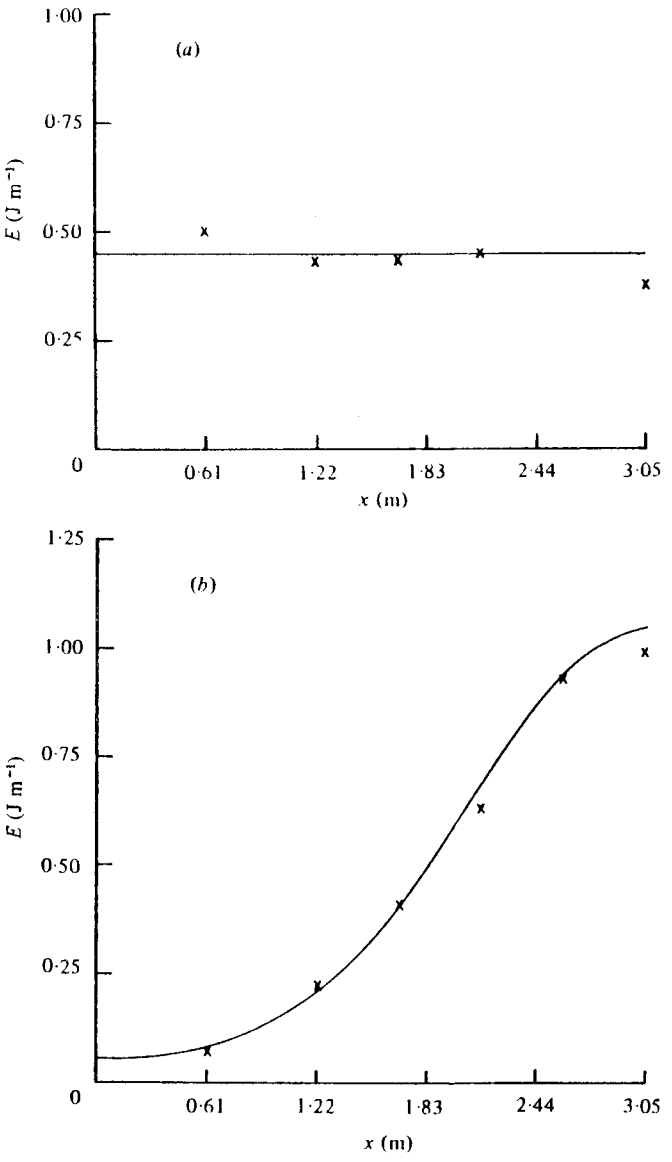

FIGURE 7. The potential energy flux: (*a*) at $y = 5{\cdot}80$ for $T = 2$, $MAD = 4{\cdot}0\,\%$; (*b*) at $y = 18{\cdot}90$ for $T = 2$ s, $MAD = 2{\cdot}6\,\%$.

can be solved numerically by the standard Crank–Nicholson method. The distribution of the potential $V(x, y)$, which is always non-negative, is shown in figure 5. In figure 6 we present the contour lines for $|\bar{F}^{(0)}|^2$ period, $T = 3$ s. It is interesting to point out that the feature of two interesting waves near the downstream corners of the tank ($y \geqslant 22{\cdot}0$) is captured (see figures 4 and 6).

In Whalin's work (1971), for each of the periods $T = 1, 2, 3$ s a set of three distinct wave amplitudes (here referred to as $AMP = 1, 2, 3$ in the increasing order of magnitude) was tested. For a given period and amplitude there were recorded three sets of data (A, B, C) with different arrangements of the locations of a total of twenty wave

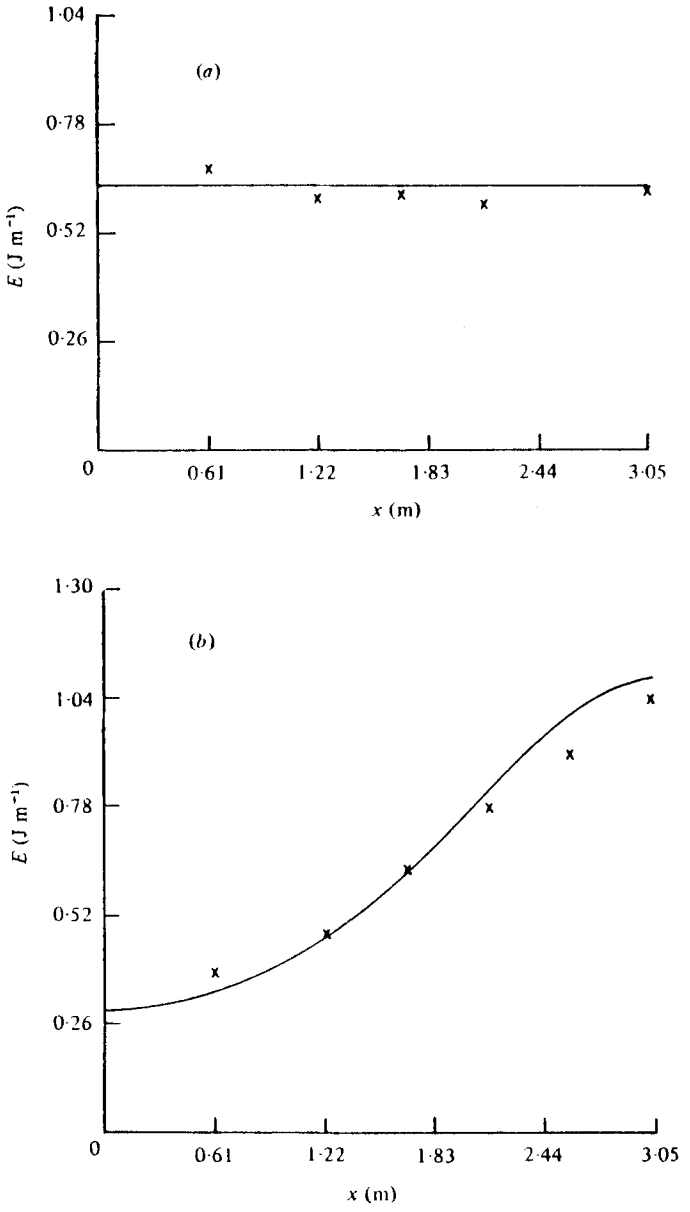

FIGURE 8. The potential energy flux: (*a*) at $y = 5{\cdot}80$ for $T = 3$ s, $MAD = 2{\cdot}3\,\%$; (*b*) at $y = 18{\cdot}90$ for $T = 3$ s, $MAD = 3{\cdot}6\,\%$.

gauges. The wave-gauge stations 1–6 were always located along a straight line $y =$ constant in the constant water depth region between the wave-maker and the first semicircular step. Wave-gauge stations 7–12 were positioned along the perimeter of one of the semicircular steps; different steps were chosen for different experimental set-ups (A, B, C). The gauge stations 13–20 were installed in the region of shallower constant water depth. Detailed information concerning the locations of wave gauges is referred

Station number	Co-ordinates (m)		Potential energy flux, E (J m^{-1})			
			$T = 2$ s		$T = 3$ s	
	x	y	Experiment	Theory	Experiment	Theory
7	3·048	12·95	0·59	0·57	0·74	0·80
8	2·590	13·00	0·47	0·55	0·73	0·80
9	2·133	13·10	0·57	0·51	0·49	0·78
10	1·676	13·30	0·45	0·44	0·66	0·74
11	1·219	13·60	0·35	0·36	0·57	0·57
12	0·609	14·20	0·27	0·27	0·36	0·43

TABLE 1. Comparisons between theoretical results and experimental data.

to Whalin (1971). The reported data (see Whalin 1971, p. 40, table 6) was the potential energy flux over a period, which can be expressed in terms of our notations as follows:

$$E(x,y) = \tfrac{1}{2}\rho g C_g \int_0^T \eta^2\,dt = \frac{T}{4}\rho g |\bar{F}^{(0)}|^2 \cosh^2 \bar{k}_0 \bar{h}_0. \tag{4.10}$$

In figures 7–8, we present the theoretical results (solid line) and experimental data (experimental set-up B, $AMP = 1$, Whalin 1971) of the potential energy flux at cross-sections $y = 5{\cdot}80$ and $18{\cdot}90$ for $T = 2$ and 3 s, respectively. As mentioned before the wave-gauge stations 7–12 were positioned along the perimeter of one of the semicircular steps. For the experimental set-up B, the locations of these wave gauges and experimental data of the potential energy flux are tabulated in table 1 for $T = 2$ and 3 s, respectively. The corresponding theoretical results are also listed in the table. Similar comparisons have been performed for the experimental set-ups A and C and can be found in Lozano (1979). The experimental data for $T = 1$ s is not used for comparison because in this case the reflexions from the semicircular steps become significant, which violates the basic assumption used in the theory.

The relative error between the theoretical results and experimental data as shown in figures 7–8 is defined as follows

$$MAD = \left(\sum_{j=1}^{N} |E_j - \overset{0}{E}_j|^2\right)^{\frac{1}{2}} / N\langle E\rangle, \tag{4.11}$$

where E_j and $\overset{0}{E}_j$ represent the theoretical and experimental potential energy flux at each wave-gauge station, respectively; $\langle E\rangle$ denotes the average of the theoretical values at a cross-section (y = constant), and N is the number of wave-gauge stations along the cross-section. In figures 7 and 8, all the relative errors are within 5 %. The over all general qualitative agreement between the theoretical results and experimental data is reasonably good. We should point out that the cross-section $y = 18{\cdot}9$ cuts across the caustics and the shadow region (see figure 4). As shown in figures 7(*b*) and 8(*b*) the parabolic approximation indeed predicts the wave focusing near the centre-line (caustic) and the wave decaying into the shadow region.

5. Concluding remarks

In this paper we have derived a parabolic approximation for studying combined refraction and diffraction problems based on linear water wave theory. The parabolic approximation accounts for both transversal diffusion of wave amplitude across wave rays and wave ray curvature. Theoretically we show that the leading-order solution of the parabolic approximation has a uniform error $O(\delta^{\frac{1}{3}})$, where δ characterizes the mild slope, and the leading approximation is valid in regions at a distance $O(\delta^{-\frac{4}{3}})$ from the given initial wave front. Two simple problems are employed in the paper to demonstrate the applicability of the method in that it is relatively easy to obtain solutions. We hope that after more systematic verification of the present theory by controlled laboratory experiments, the parabolic approximation can be used as an efficient tool for describing linear water wave refraction and diffraction.

This research was supported in part by the Sea Grant Research Program at the University of Delaware and at Cornell University. The authors would like to thank Dr Robert G. Dean and Dr Robert Whalin for their stimulating discussions on the subject.

Appendix

Introducing the following notations and operators

$$\tilde{F}_{\tilde{\sigma}} = h_{(\tilde{\sigma})}^{-1}\frac{\partial \tilde{F}}{\partial \tilde{\sigma}}, \quad \tilde{F}_{\tilde{\rho}} = h_{(\tilde{\rho})}^{-1}\frac{\partial \tilde{F}}{\partial \tilde{\rho}}, \tag{A 1}$$

$$\Delta_{(\tilde{\sigma})}\tilde{F} = h_{(\sigma)}^{-2}\frac{\partial^2 F}{\partial \tilde{\sigma}^2} + [h_{(\sigma)}h_{(\rho)}]^{-1}\left[\frac{\partial (h_{(\rho)}h_{(\sigma)}^{-1})}{\partial \tilde{\sigma}}\right]\frac{\partial \tilde{F}}{\partial \tilde{\sigma}}, \tag{A 2}$$

$$\Delta_{(\rho)}\tilde{F} = h_{(\rho)}^{-2}\frac{\partial^2 \tilde{F}}{\partial \tilde{\rho}^2} + [h_{(\rho)}h_{(\sigma)}]^{-1}\left[\frac{\partial (h_{(\sigma)}h_{(\rho)}^{-1})}{\partial \tilde{\rho}}\right]\frac{\partial \tilde{F}}{\partial \tilde{\rho}}, \tag{A 3}$$

$$G(A) = A_{zz}\cosh\zeta + 2kA_z\sinh\zeta, \tag{A 4}$$

$$H(A) = (\Delta S)A\cosh\zeta + 2\nabla S\,.\,\nabla(A\cosh\zeta), \tag{A 5}$$

and substituting (2.19)–(2.27) into (2.16)–(2.18), we obtain

$$\begin{aligned}
&\{[k^2-(\nabla S)^2]\,\tilde{F}a\cosh\zeta\} + \epsilon^3\{\tilde{F}[G(A^{(0)}) + iH(a)]\}\\
&+\epsilon^4\{[2ik\tilde{F}_{\tilde{\sigma}}^{(0)} + \Delta_{(\tilde{\rho})}\tilde{F}^{(0)}]\,a\cosh\zeta\}\\
&+\epsilon^5\{[2ik\tilde{F}_{\tilde{\sigma}}^{(1)} + \Delta_{(\tilde{\rho})}\tilde{F}^{(1)}]\,a\cosh\zeta + 2\tilde{F}_{(\tilde{\rho})}^{(0)}\,\mathbf{n}\,.\,\nabla(a\cosh\zeta) + \tilde{F}_{\tilde{z}\tilde{z}}^{(1)}\,a\cosh\zeta\}\\
&+\epsilon^6\{\tilde{F}^{(0)}[G(A^{(1)}) + iH(A^{(0)}) + \Delta(a\cosh\zeta)]\\
&\quad + 2\tilde{F}_{\tilde{\rho}}^{(1)}\,\mathbf{n}\,.\,\nabla(a\cosh\zeta) + \tilde{F}_{\tilde{z}\tilde{z}}^{(2)}\,a\cosh\zeta + 2(A^{(0)}\cosh\zeta)_z\,\tilde{F}_{\tilde{z}}^{(1)}\\
&\quad + [2ik\tilde{F}_{\tilde{\sigma}}^{(2)} + \Delta_{(\tilde{\rho})}\tilde{F}^{(2)}]\,a\cosh\zeta\} + O(\epsilon^7) = 0, \quad -h \leqslant z \leqslant 0;
\end{aligned} \tag{A 6}$$

$$\begin{aligned}
&\tilde{F}a[k\sinh kh - \cosh kh]\\
&+\epsilon^3\{\tilde{F}[A^{(0)}(k\sinh kh - \cosh kh) + A_{\tilde{z}}^{(0)}\cosh kh] + \tilde{F}_{\tilde{z}}^{(1)}\,a\cosh kh\}\\
&+\epsilon^4\tilde{F}_{\tilde{z}}^{(2)}\,a\cosh kh + \epsilon^5\tilde{F}_{\tilde{z}}^{(3)}\,a\cosh kh\\
&+\epsilon^6\{\tilde{F}^{(0)}[A^{(1)}(k\sinh kh - \cosh kh) + A_{\tilde{z}}^{(1)}\cosh kh]\\
&\quad + \tilde{F}_{\tilde{z}}^{(4)}\,a\cosh kh + \tilde{F}_{\tilde{z}}^{(0)}A^{(0)}\cosh kh\} + O(\epsilon^7) = 0, \quad z = 0;
\end{aligned} \tag{A 7}$$

$$\epsilon^3\{\tilde{F}[A_z^{(0)}+i(\nabla S\,.\,\nabla h)\,a]+a\tilde{F}_z^{(2)}\}$$
$$+\epsilon^4\tilde{F}_z^{(2)}\,a+\epsilon^5\{[\tilde{F}_z^{(3)}+h_\rho\tilde{F}_\rho^{(0)}]\,a\}$$
$$+\epsilon^6\{\tilde{F}^{(0)}[A_z^{(1)}+i(\nabla S\,.\,\nabla h)\,A^{(0)}+\nabla h\,.\,\nabla a]+\tilde{F}_z^{(4)}a$$
$$+\tilde{F}_z^{(1)}A^{(0)}\}+O(\epsilon^7)=0,\quad z=-h. \tag{A 8}$$

Equating the coefficients of each power of ϵ to zero, we obtain the following sequence of problems:

$O(\epsilon^0)$:

$$k^2-(\nabla S)^2=0;\quad k\tanh kh=1. \tag{A 9), (A 10}$$

$O(\epsilon^3)$:

$$A_{zz}^{(0)}\cosh\zeta+2kA_z^{(0)}\sinh\zeta+i(\Delta S)\,A^{(0)}\cosh\zeta$$
$$+2\nabla S\,.\,\nabla(A^{(0)}\cosh\zeta)=0,\quad -h<z<0; \tag{A 11}$$
$$A_z^{(0)}=a\tilde{F}_z^{(1)}/\tilde{F}^{(0)},\quad z=0; \tag{A 12}$$
$$A_z^{(0)}+i(\nabla S\,.\,\nabla h)\,a=a\tilde{F}_z^{(1)}/\tilde{F}^{(0)},\quad z=-h. \tag{A 13}$$

$O(\epsilon^4)$:

$$2ik\tilde{F}_\sigma^{(0)}+\Delta_{(\tilde{\rho})}\tilde{F}^{(0)}=0,\quad -h<z<0; \tag{A 14}$$
$$\tilde{F}^{(1)}A_z^{(0)}+\tilde{F}_z^{(2)}a=0,\quad z=0; \tag{A 15}$$
$$F^{(1)}[A_z^{(0)}+i(\nabla S\,.\,\nabla h)\,a]+a\tilde{F}_z^{(2)}=0,\quad z=-h. \tag{A 16}$$

The $O(\epsilon^0)$ problem confirms the wave ray pattern according to the geometrical optics theory. The $O(\epsilon)$ and $O(\epsilon^2)$ problems provide no additional information. The $O(\epsilon^3)$ problem indicates that if the leading wave action a indeed satisfies the transport equation (2.8) based on the ray theory, then

$$A_z^{(0)}=0,\quad \tilde{F}_z^{(1)}=0\quad \text{for}\quad z=0, \tag{A 17}$$
$$A_z^{(0)}+i(\nabla S\,.\,\nabla h)\,a=0,\quad \tilde{F}_z^{(1)}=0\quad \text{for}\quad z=-h, \tag{A 18}$$

which leads to the boundary conditions for $\tilde{F}^{(1)}$. In $O(\epsilon^4)$ problem, (A 14) constitutes the leading-order approximation for the diffraction factor $\tilde{F}^{(0)}$. The governing equation for the diffraction factor $\tilde{F}^{(1)}$ can be found in $O(\epsilon^5)$ problem, i.e.,

$$[2ik\tilde{F}_\sigma^{(1)}+\Delta_{(\tilde{\rho})}\tilde{F}^{(1)}+\tilde{F}_{zz}^{(1)}]\,a\cosh\zeta=-2\tilde{F}_\rho^{(0)}\,\mathbf{n}\,.\,\nabla(a\cosh\zeta). \tag{A 19}$$

REFERENCES

Candel, S. M. 1979 *J. Fluid Mech.* **90**, 465–507.

Chao, Y.-Y. 1971 *J. Geophys. Res.* **76**, 7401–7407.

Keller, J. B. 1958 *J. Fluid Mech.* **4**, 607–614.

Kriegsmann, G. A. & Larsen, E. W. 1978 *SIAM J. Appl. Math.* **34**, 200–204.

LeBlond, P. H. & Mysak, L. A. 1978 *Waves in the Ocean*. Elsevier.

Liu, P. L-F. & Mei, C. C. 1976 *J. Geophys. Res.* **81**, 3079–3084.

Liu, P. L.-F., Lozano, C. J. & Pantazaras, N. 1979 *J. Appl. Ocean Res.* **1**, 147–157.

Lozano, C. J. 1979 *Appl. Math. Inst. Univ. Delaware, Newark De, Tech. Rep.* no. 25.

Ludwig, D. 1964 *Comm. Pure Appl. Math.* **19**, 215–250.

Mei, C. C. & Tuck, E. O. 1980 *SIAM J. Appl. Math.* (to appear).

Shen, M. C. 1972 In *Waves on Beaches* (ed. by R. E. Meyer). Academic.

Shen, M. C. & Keller, J. B. 1975 *SIAM J. Appl. Math.* **28**, 857–875.

Wehausen, J. & Laitone, E. 1960 In *Handbuch der Physik*, IX-3. Springer.

Whalin, R. W. 1971 *U.S. Army Engng Waterways Expt. Station, Vicksburg, Mi, Res. Rep.* H71-3.